Mechanics of Advanced Composite Structures 13 (2026), Serial Number 27, 197 – 210

Mechanics of Advanced Composite Structures

Journal homepage: https://macs.semnan.ac.ir/

Semnan University

ISSN: 2423-7043

Research Article

Reinforcement Surface Modification Effect on the Microstructure, Mechanical, and Tensile Fractography of Al2219 Alloy B_4C Composites

Subhashchandra Ganiger [a], Mahadev Sakri [a], Naveen Kumar Bannuru Karagaiah [b], Halkur Siddagangaiah Kumar [c]*, Manjunath Yadav Siriyanna [d], Vijayendra Kukanur [e], Madeva Nagaral [f], Fazil Nalband [g], Virupaxi Auradi [h], Nagaraj Namdev [i]

[a] *Department of Mechanical Engineering, B.L.D.E.A's Dr. P. G. Halakatti College of Engineering and Technology, Vijayapur-586103, Karnataka, India*

[b] *Department of Mechanical Engineering, M S Ramaiah Institute of Technology, Bengaluru, India*

[c] *Department of Mechanical Engineering, Nitte (Deemed to be University), NMAM Institute of Technology, Karkala-574110, Karnataka, India*

[d] *Department of Mechanical Engineering, Government Engineering College, Gangavathi-583227, Karnataka, India*

[e] *Department of Mechanical Engineering, H.K.E. Society's SiR M. Visvesvaraya College of Engineering, Raichur-584135, Karnataka, India*

[f] *Aircraft Research and Design Centre, Hindustan Aeronautics Limited, Bangalore-560037, Karnataka, India*

[g] *Department of Mechanical Engineering, Ballari Institute of Technology and Management, Ballari, Karnataka, India*

[h] *Department of Mechanical Engineering, Siddaganga Institute of Technology, Tumakuru-572103, Karnataka, India*

[i] *Department of Mechanical Engineering, APS Polytechnic, Bangalore-560082, Karnataka, India*

ARTICLE INFO

Article history:

Received: 2024-07-28
Revised: 2025-07-29
Accepted: 2025-08-28

Keywords:

Al Alloy;
Boron carbide;
Stir castingl;
Electroless coating;
Tensile ctrength.

ABSTRACT

Al2219 alloy composites were produced through the stir cast process, with varying amounts of copper-coated B_4C particles (2%, 4%, 6%, 8%, and 10%) incorporated. The mechanical performance of surface-modified B_4C additions to Al2219 alloy was examined by conducting tensile tests on the prepared composites. The synthesized composites' microstructural, mechanical, and tensile fractured surfaces were evaluated. Characterization of the samples' microstructure using SEM microscopy and EDS patterns. B_4C particle existence was verified by the EDS findings. The inclusion of Cu-coated B_4C reinforcement enhanced the hardness, tensile, and bending strength of the metal composite in contrast to the uncoated B_4C particles. Hardness of Al2219 alloy was improved by 92.4% with the 10 wt.% of Cu coated B_4C in the Al matrix. Further, there was a 73.5 % improvement in the ultimate strength. The Al2219 alloy composite's ductility decreased with the reinforcement's incorporation. Tensile fractured surfaces SEM micrographs show strong bonding between the matrix and boron carbide particles. The particle shear was observed in the case of copper-coated B_4C reinforced composites due to increased wettability. Various fractured surfaces were studied using SEM micrographs to determine fracture mechanisms in composites.

* **Corresponding author.**
E-mail address: urkumar2006@nitte.edu.in

Cite this article as:

Ganiger, S., Sakri, M., Karagaiah, N.K.B., Kumar, H.S., Siriyanna, M.Y., Kukanur, V., Nagaral, M., Nalband, F., Auradi, V., Namdev, N., 2026. Reinforcement Surface Modification Effect on the Microstructure, Mechanical, and Tensile Fractography of Al2219 Alloy B_4C Composites. *Mechanics of Advanced Composite Structures*, 13(1), pp. 197-210.

https://doi.org/10.22075/MACS.2025.34881.1705

1. Introduction

The automotive and aerospace industries are using MMC more and more due to its lightweight, high strength-to-weight ratio, high modulus-to-weight ratio, and enhanced wear resistance. [1–3]. Metal matrix composites (MMCs) with an aluminium basis are well-known for having superior mechanical qualities, low density, low CTE, and ease of fabrication [4]. Applications for Al-based MMCs include engine pistons, cylinder liners, and brake discs/drums [5]. Adding ceramic particles to the Al matrix strengthens and improves its characteristics [6-8]. Various methods can be employed to produce Al-based MMCs, including squeeze casting, powder metallurgy, stir casting, and spray deposition. [8]. Casting, the most cost-effective and versatile processing method, is preferred. During conventional stir casting, strong ceramic reinforcements are added to the melt vortex and transmitted to the permanent mould [9].

Many studies believe that selecting adequate processing parameters might address uniform distribution and bonding issues. Currently, most Al-based MMC investigations focus on SiC and Al_2O_3 particle reinforcements, with minimal utilisation of B_4C particulates in the Al matrix. B4C, known as the third hardest material, has a lot of potential applications in such as bulletproof vests, armour tanks, and neutron absorbers [10,11]. B_4C has a low density of 2.52 g/cc, comparable to Al matrix, and high stiffness (445 GPa) and hardness (3700 Hv) [12]. The use of B_4C as reinforcement is limited by its high cost and lower wettability by molten Al below 1100 °C [13]. Low wettability of reinforcement prevents liquid Al from fully covering B_4C particles. Particles float on the melt surface due to increased surface tension and reinforcing interfacial forces [14].

The interaction between matrix and reinforcement substantially affects MMC characteristics. Since the Al matrix alloy is a metal, and boron carbide particles are non-metal, it is always very difficult to have these particles within the metal matrix. Wettability of matrix and reinforcement is the key factor affecting interfacial characteristics [15]. Lack of wettability, chemical reactivity, and reinforcement deterioration result from improper interface tailoring. The required interface is achieved by surface treating reinforcement, coating it, optimizing process parameters, and changing matrix composition. Coating is a crucial method for enhancing interfaces that are extensively studied [16, 17]. Thus, this study aims to transform the surface of ceramic particles into a metallic state by applying a copper coating. This process facilitates direct contact between metals and enhances their ability to be wetted. Adhesion of molten matrix material to the reinforcing surface is limited by the coating. Chemical reactivity at the contact is minimized without diffusion [18]. Wetness of reinforcement in the molten matrix is also increased by coating. Coating reinforcement particles include chemical, physical, thermal, electroless, and electrolytic deposition. Electroless deposition and its quick setup, cheap cost, uniform, and continuous coating are making it popular [19, 20].

It is always difficult to have the proper bonding between the metal and ceramic particles during the preparation of metal composites. To increase the wettability between the matrix and ceramic reinforcement, in the present study, carbide particles are coated with copper, so that the ceramic particle's surface has been converted into a metal surface. Copper-coated B_4C particles play an important role in enhancing the wettability. This study synthesizes Al2219-based composites with reinforcements of uncoated B_4C / Cu-coated B_4C particles with 2, 4, 6, 8, and 10 wt.% using a unique two-stage stir casting process and studies the MMC's mechanical properties.

2. Experimental Details

2.1. Materials Used

Al2219 was the basis, and micro-B_4C the reinforcement. A support particle, B_4C, has a theoretical density of 2.52 g/cm^3, and grid material Al2219 amalgam 2.80 g/cm^3. Table 1 shows the Al2219 composite chemistry used in this work.

Table 1. Chemistry of Al2219 alloy

Elements	Percentage
Magnesium	0.01
Silicon	0.15
Iron	0.28
Copper	6.77
Titanium	0.10
Zirconium	0.10
Zinc	0.10
Manganese	0.02
aluminum	Remaining

Figure 1 shows that the present study uses 80–90 micron B_4C particles as strengthening materials. The matrix material has 2.52 g/cm^3, while B_4C has less density. Electroless coating uses copper to coat boron carbide particles.

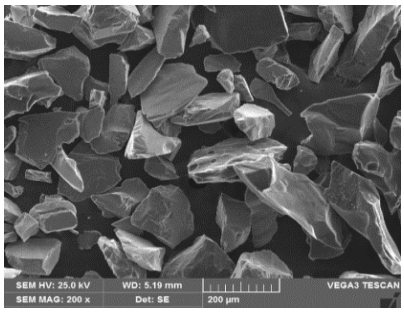

Fig. 1. SEM micro-photograph of 80- 90 micron-sized B_4C

2.2. Preparation of Composites

A liquid metallurgy process and stir casting produced 80-90 micron Al2219-B4C composites. A certain number of Al2219 compound ingots are liquefied in the furnace. Aluminium alloys melt at 660°C. The liquid reached 750oC. A chrome-alumel thermocouple will record temperature. The liquid metal is then degassed for 3 minutes with solid hexachloroethane (C_2Cl_6) [21]. A tempered steel impeller coated with zirconium mixes liquid metal to create a vortex. The stirrer will spin at 300 rpm and the impeller will be immersed to 60% of the liquid metal's height from the liquefy's exterior. A heater will heat the copper-coated B_4C particles to 500°C before they enter the vortex. Stirring continues until the support particles and network interface communications reach dampness. The Al2219-2 wt. % B_4C combination is then cast into a durable 120 mm x 15 mm cast iron form. Materials composed of a matrix reinforced with B4C particles with 4, 6, 8, and 10% content are also made. ASTM (American Society for Testing and Materials). Guidelines were used to calculate the mechanical properties created in the microstructural research. An Al2219 alloy reinforcement particulate dispersion research is conducted using a scanning electron microscope after the specimen has been cast.

Densities of Al2219 alloy with copper-coated and uncoated B4C composites were examined. Experimental densities were compared to theoretical values using the usual weight method and the rule of mixture to estimate theoretical values. Hardness is tested using ASTM E10 by using a Brinell hardness tester [22]. Every prepared sample underwent testing for different specimens, and the average value was plotted.

Tensile testing was performed on Al2219 alloy samples with different percentages of uncoated and copper-coated B4C particle reinforced composites machined according to ASTM standard E8 [23]. The specimen has a 104-mm length, 45-mm gauge, and 9-mm diameter. A tensile test determines a material's ultimate strength, yield strength, and elongation. Compressive strength is evaluated using ASTM E9. The experiment's tensile specimen is presented in Figure 2.

Fig. 2. Tensile test specimen

3. Results and Discussion

3.1. Microstructural Analysis

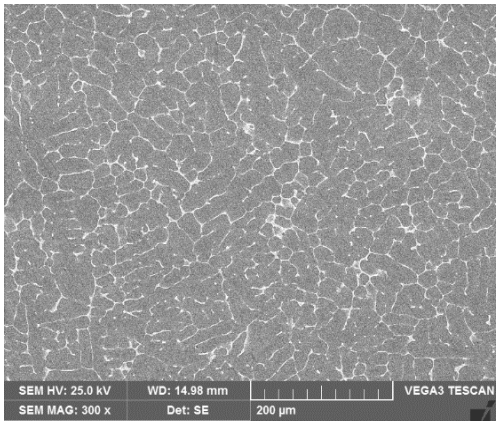

(a)

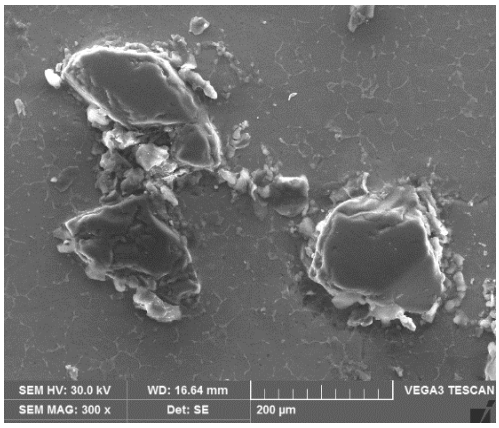

(b)

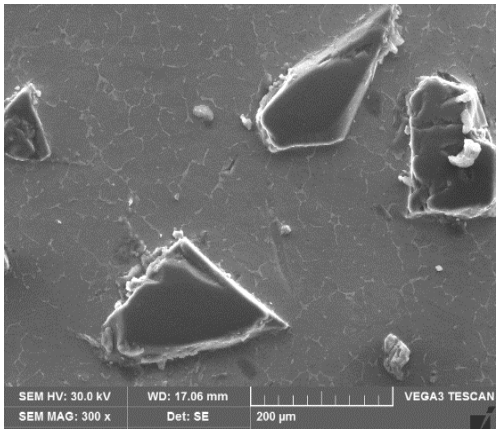

(c)

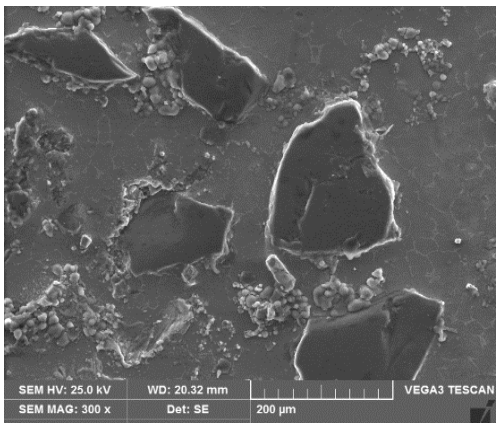

(d)

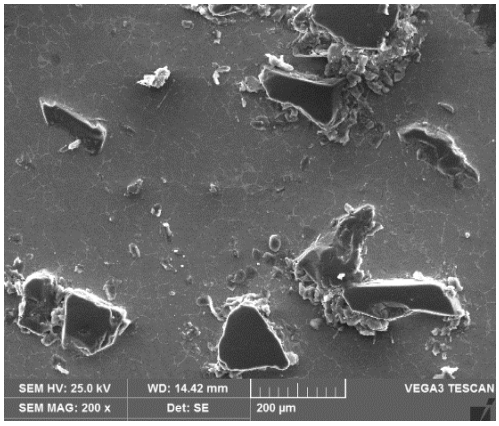

(e)

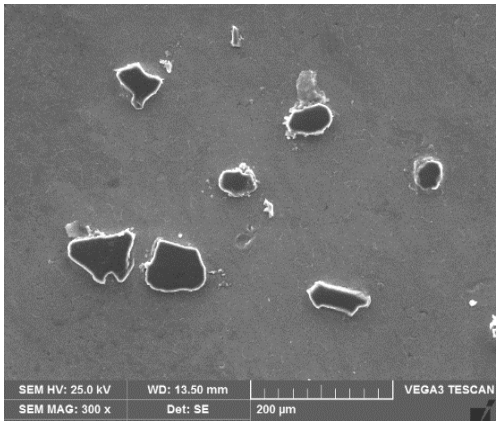

(f)

Fig. 3. SEM of : (a) as cast Al2219 alloy, (b) Al2219-2% B_4C, (c) Al2219-4% B_4C, (d) Al2219-6% B_4C, (e) Al2219-8% B_4C, (f) Al2219-10% B_4C composites without coating

Figure 3 (a-f) shows composite SEM images without and with coating reinforced by Al2219 alloy and micro B_4C particles. Figure 3 (a) shows a pure Al2219 alloy SEM. Figure 3 (b-f) displays Al2219 with 2–10 wt. % B_4C composites SEM picture. Make sure the Al2219 alloy evenly mixes the % micro-B_4C composite or most micro-B_4C particles. The composite material created is uniform in these figures.

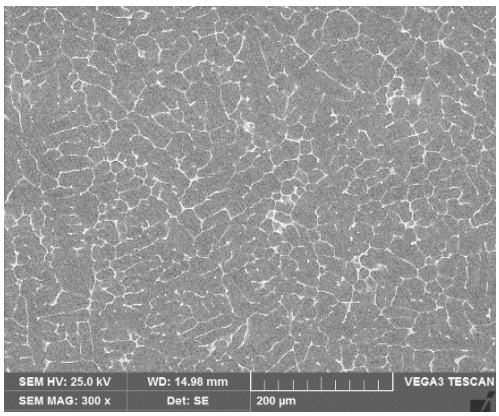

(a)

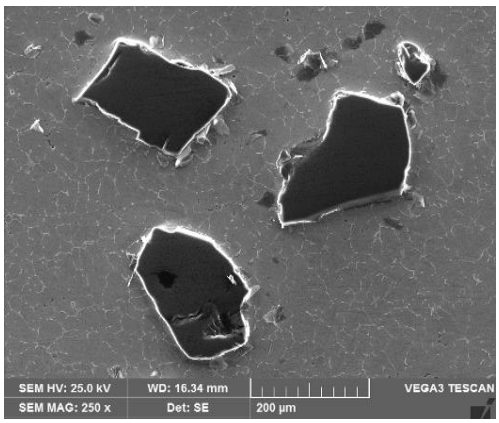

(b)

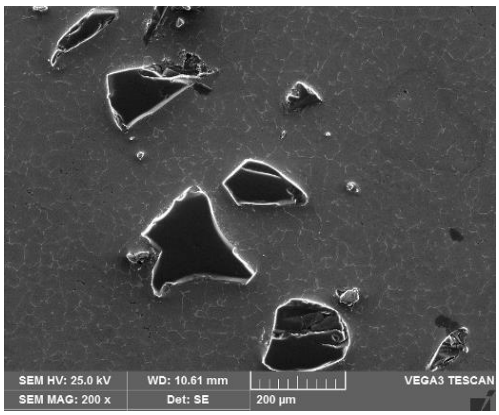

(c)

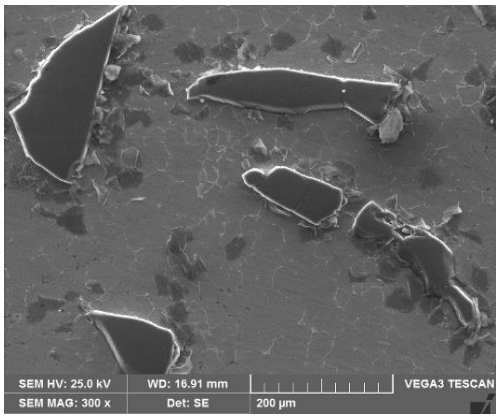

(d)

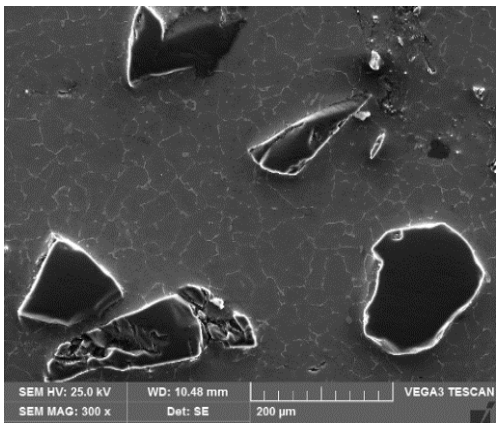

(e)

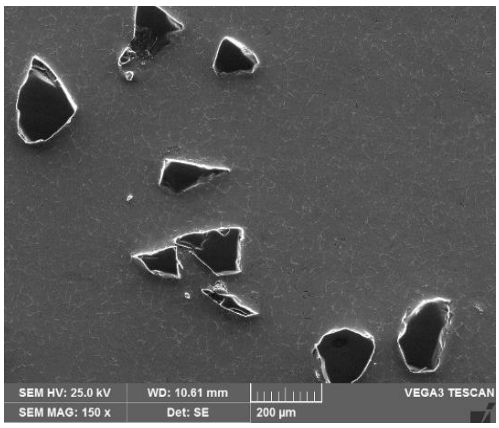

(f)

Fig. 4. SEM of (a) as cast Al2219 alloy, (b) Al2219-2% B_4C, (c) Al2219-4% B_4C, (d) Al2219-6% B_4C, (e) Al2219-8% B_4C, (f) Al2219-10% B_4C composites with copper coating

Figure 4 (a-f) shows SEM images of copper-coated B_4C-reinforced composites and Al2219 alloy. This matches Figure 4 (a), which displays a pure Al2219 alloy SEM. Figure 4 (b-f) shows Al2219 with 2–10 wt.% B_4C composites and copper-coated particles. B_4C particles in Al2219 alloy are equally dispersed. These figures also demonstrate composite homogeneity.

Copper-coated B_4C particles were injected after two phases into the Al2219 matrix, as illustrated in Figure 4 (b-f), improving matrix-particle bonding. Copper-coated B4C particles improve matrix wettability in Al2219 alloy composites. In Figure 4 (b-f), the tiny B_4C particle bonds strongly to the aluminium Al2219 matrix. Wetting ceramic particles with metal is challenging, but in this research, the ceramic particles were coated in copper to give them a metal appearance. This copper coating on boron carbide particles improves metal-metal surface interaction and wettability. Thus, improved wettability ensures a stable matrix-reinforcement interface without voids or microcracks [24, 25].

Figure 5, the Al2219 alloy's EDS spectrum displays the primary alloying elements Cu, Si, Fe, Mn, and Mg in the Al matrix. Figures 6 (a) and 6 (b) exhibit Al2219-10 wt.% B_4C without Cu coating composite and with Cu-coated B_4C particles. For Al2219 – 10% B_4C reinforced composites, coated and not coated, EDS analysis confirms B_4C as a C component.

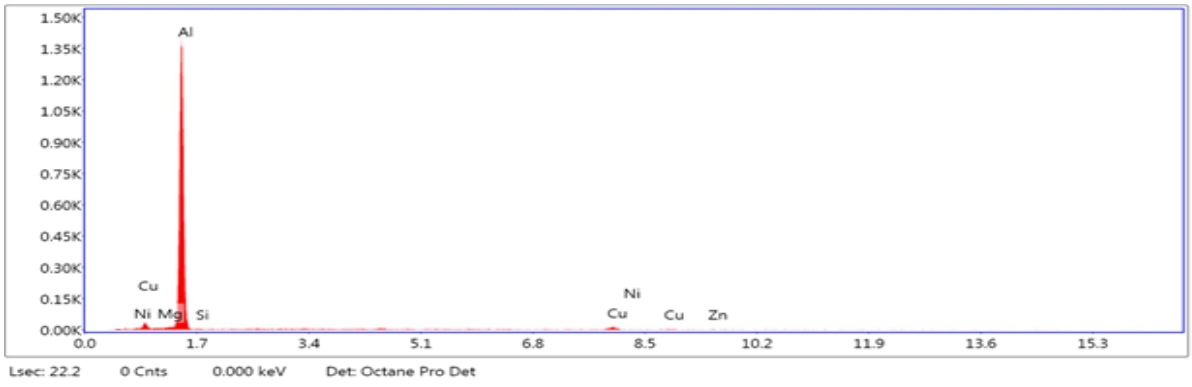

Fig. 5. EDS of as-cast Al2219 alloy

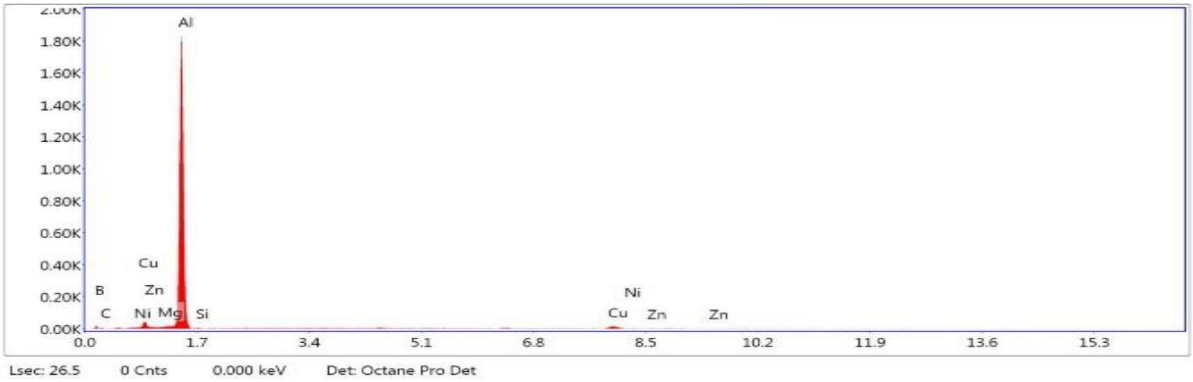

(a)

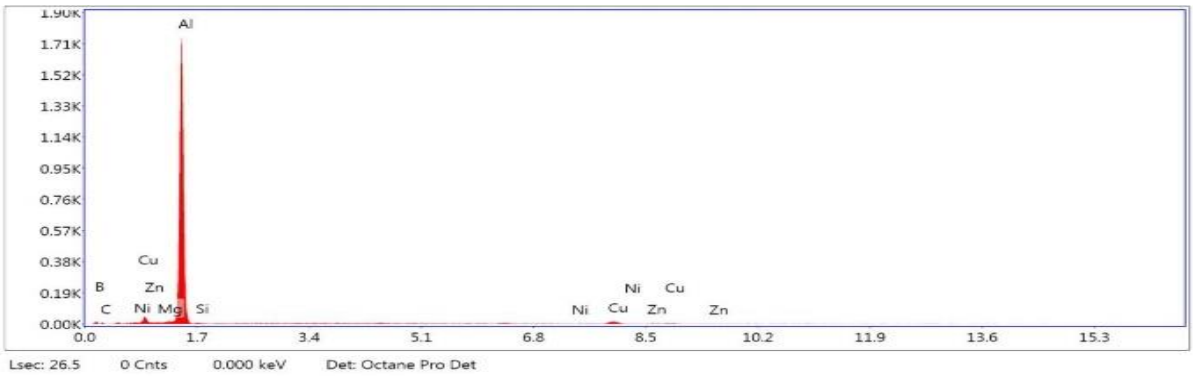

(b)

Fig. 6. EDS of (a) Al2219-10% B4C composites uncoated, (b) Al2219-10% B4C composites with Cu coating

3.2. Density Measurements

Al2219, Al2219-2, 4, 6, 8, and 10% Figure 7 displays micro B_4C composites. Displayed are theoretical and experimental values for each sample. Because the theoretical values estimated are related to the practical values obtained experimentally, this study's experimental values should match the theoretical values. Since calculating theoretical values is done with established methods, experimental outcomes rarely match theoretical values. The weight method determines the density of Al2219, Al2219-2, 4%, 6%, 8%, and 10% B_4C composites.

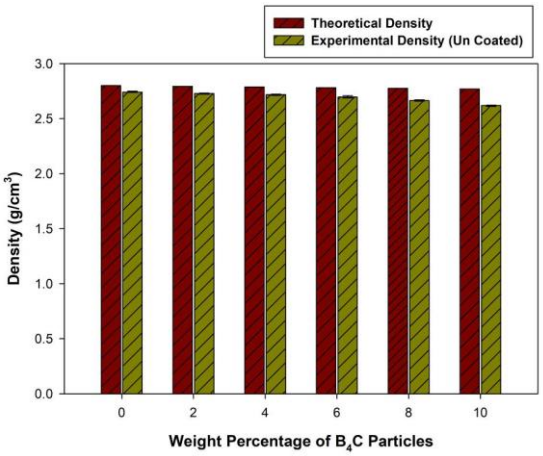

Fig. 7. The densities of Al2219-B_4C Composites without coatings of B_4C particles

Figure 7 shows Al2219 with 2 wt.% B_4C, 4 wt.%, 6 wt.%, 8 wt.%, and 10 wt.% uncoated B4C composites. Aluminium alloy Al2219 has a density of 2.80 g/cm3, boron carbide 2.52, and Al alloy with 2% B4C 2.794. B_4C has a lower density than Al2219 alloy, reducing the composite's density. When B_4C particles make up 4, 6, or 10% of the Al2219 alloy, the composite's theoretical density is lower than the aluminium alloy's. Also, real densities are lower than expected. Boron carbides decrease density, according to other experts [26].

Figure 8 compares cast Al2219 alloy to 2–10% Cu-coated B_4C reinforced composites. According to Figure 8, the experimental density falls as the weight percent of Cu-coated B_4C particles in Al2219 alloy increases. Al2219 alloy with 10% B_4C composites reinforced with particles has a 2.631 g/cm^3 density, compared to 2.74 g/cm^3 for the as-cast alloy. Al2219-B_4C composites exhibit a lower density compared to the Al2219 alloy matrix because B_4C particles are lighter.

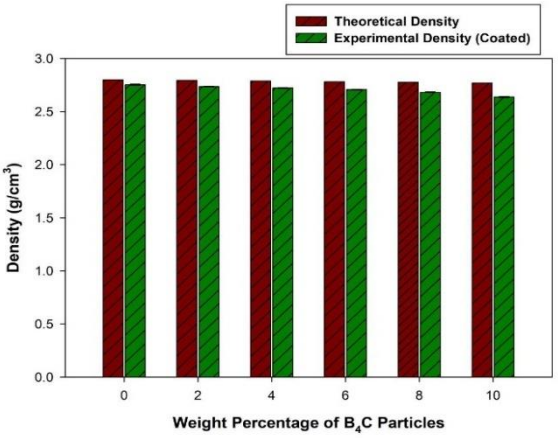

Fig. 8. Densities of theory and experiment of Al2219-B_4C composites with Cu coated B_4C particles

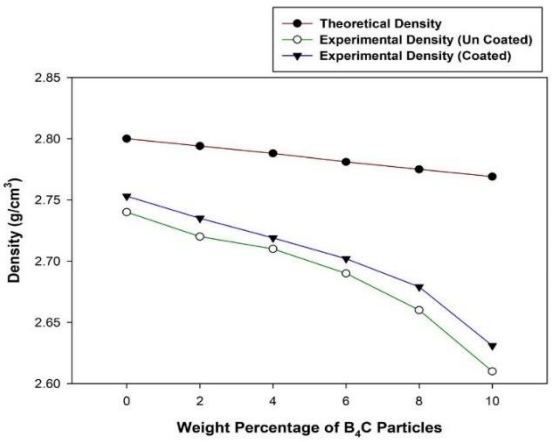

Fig. 9. Al2219 alloy experimental densities when comparing composites reinforced by uncoated and Cu-coated B_4C particles

Figure 9 illustrates an assessment of the densities of Al2219 alloy reinforcement of composites with not coated and Cu-coated B4C particles, both in theoretical and practical terms. It is always challenging to align the theoretical and practical density. Experimental density will be less dense than it should be due to the contraction of the cast sample. Theoretical densities of not-coated and Cu-coated particle-reinforced composites exceed the observed densities. The sound casting procedure used to make composites minimises the difference. Cu-coated B_4C reinforcement with particles of Al2219 alloy composites had somewhat greater experimental densities than uncoated composites. Good reinforcement-matrix alloy bonding causes this small density increase [27, 28].

3.3. Hardness Measurements

Figure 10 indicates that Al2219 alloy hardness improves from 2% to 10% by weight with increasing percentages of uncoated B_4C particles. Al2219 became the hardest alloy in the world at 113.2 BHN with 10 wt. % uncoated B_4C particles. Al2219's hardness increases by 81.4% when 10% uncoated $B4C$ particles are used. Solid B_4C particles hinder Al2219 matrix dislocations. After adding fine particles, strain energy at B_4C particle edges increases, enhancing composite hardness.

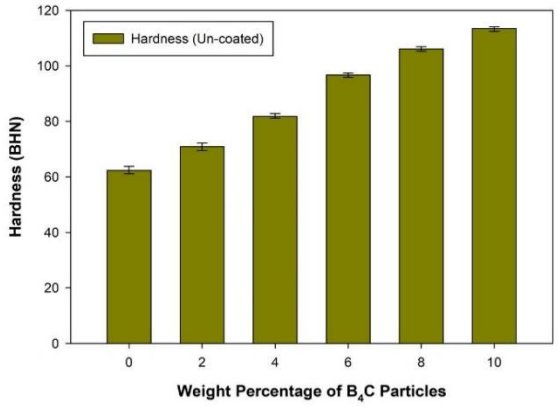

Fig. 10. Displays the hardness of Al2219 alloy reinforcement of composites with uncoated B_4C particles

Figure 11 shows that the Al2219 alloy with Cu-coated B_4C particles is harder than the Al2219 alloy alone. B_4C particles covered with Cu improve Al2219's hardness. As cast, Al2219 alloy is 62.4 BHN hard. Al2219 with 2–10% Cu-coated B_4C reinforcement with particle composites has 76.3, 91.2, 103.2, 114.2, and 120.1 BHN hardness. Al2219 alloy hardness enhanced by 92.4% with 10 wt. % Cu coated particles. Cu-coated B4C makes Al2219 harder. In hardness testing, hard particles stop plastic deformation [29].

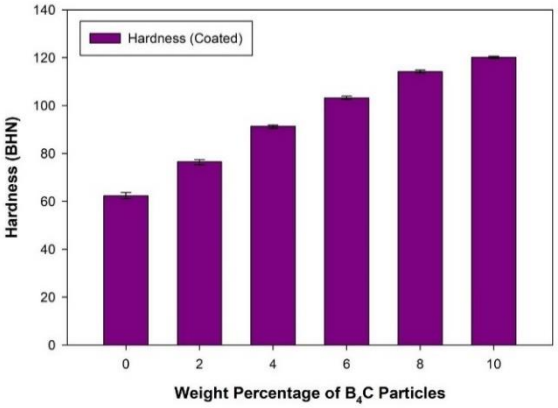

Fig. 11. Hardness of composites made of Cu-coated B_4C particles, Al2219 alloy

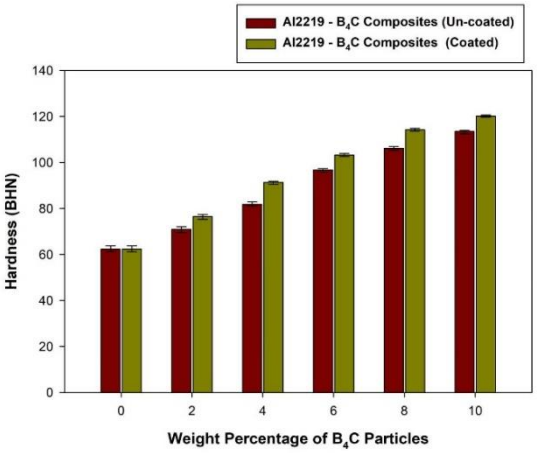

Fig. 12. Al2219 alloy's hardness in comparison to uncoated and Cu-coated B_4C reinforced composites

Figure 12 presents a study of the composite between the hardness of Al2219-B_4C with uncoated and Cu-coated B_4C particles. The graph shows that Cu-coated B_4C Composites with particles added to them are harder than uncoated ones. Uncoated B_4C reinforced Al2219-10 wt. % composite is 113.2 BHN, while the normal as-cast Al2219 alloy is 62.4 BHN. After adding 10 wt. % Cu-coated B_4C particles, Al2219 has 120.1 BHN hardness. The hardness of Al alloys with 10 wt. % uncoated and Cu-coated B_4C particles improve by 81.4 % and 92.4%, respectively. Composites with $B4C$ particles coated in Cu have a higher hardness than those without. Particles with B_4C and Cu layers make metal-to-metal contact with Al2219 alloy as an alternative to metal-ceramic contact. This metal-to-metal contact improves Al2219 alloy-ceramic particle bonding and property improvement, and also due to the homogenous distribution of Cu-Coated B_4C particles as compared to uncoated B_4C particles in matrix alloys and Al matrix particulate strengthening, Cu-Coated B_4C particles increase hardness. Hard reinforcement particles resist plastic deformation and increase composite hardness at the matrix's particle periphery due to strain energy [30, 31].

3.4. Tensile Properties

The amount of micro B_4C particles by weight utilised in tensile tests is noticeable in Figure 13. Figure 13 shows that increasing uncoated B_4C concentration in Al2219 alloy improves average UTS values. The small B_4C particle protects the Al2219 matrix alloy. As cast, Al2219 has 199.47 MPa UTS. As the fraction of micro B4C particles increases from 2% to 10% in 2% increments, UTS values rise. As noticed, Al2219 alloy with 2% uncoated B_4C composites has a UTS value of 213.4 MPa. Al2219's ultimate strength increased 51.3% with 10 wt.% micro B_4C particles without coating. The thermal expansion rate disparity between the Al2219 matrix alloy and the homogeneously dispersed micro B_4C particles increases the alloy's ultimate strength when uncoated particles (at wt.% levels of 2, 4, 6, 8, and 10) are added. Non-shearable micro B_4C in concentrations between 2 and 10 wt% strengthens Al2219 alloy by dislocation interaction. Copper plating increases particle wettability through metal-metal surface interaction.

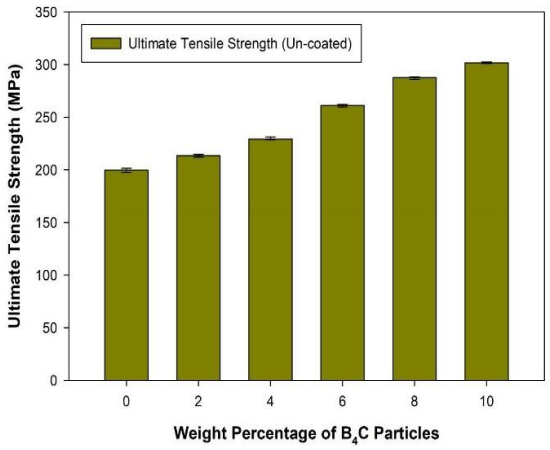

Fig. 13. Uncoated B_4C particle-reinforced Al2219 alloy composites UTS

Figure 14 shows that 2, 4, 6, 8, and 10% Cu-coated B_4C particles boost Al2219 alloy's ultimate tensile strength. As cast, Al2219 alloy has 199.47 a maximum strength. The Al2219 alloy's UTS increased with Cu-coated B_4C. Al2219 alloy reinforced composites made of 2, 4, 6, 8, and 10 wt. % Cu coated B_4C breaks the UTS at 229.25, 248.27, 281.91, 310.77, and 346.01 MPa.

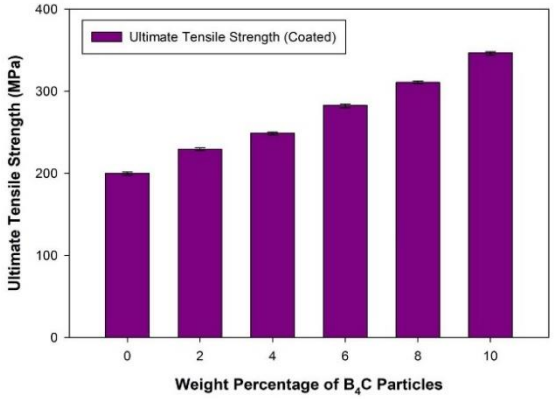

Fig. 14. UTS of Al2219 alloy reinforcement of composites made of B4C particles coated with Cu

Al2219 alloy composites reinforced by B_4C particles with and without Cu coatings are compared in Figure 15 for ultimate strength. The graph shows that when the weight percentage of coated and uncoated B_4C particles rises from 2 to 10 wt.%, the UTS of Al2219 alloy increases. Reinforced composite materials with B_4C particles coated in Cu exhibit a higher ultimate strength compared to composites that are not treated. With uncoated micro B_4C particles and 73.46% with Cu-coated particle-reinforced composites, the UTS of Al2219 increases by 51.3% and 73.46%, respectively. Hard ceramic particles typically increase the tensile strength of the soft Al matrix. Because of the strong bond between the Cu-coated reinforcement particles and the Al2219 alloy, Figure 15 demonstrates that reinforcement of composites that have Cu-coated particles results in higher UTS. The B_4C particles' surface variation allows the Cu surface and Al matrix to come into direct contact. The improved B_4C surface enhances metal-to-metal bonding and mechanical behaviour [32, 33]. The composite's mechanical characteristics improve due to its microstructure, whose particle distribution is constant, with no agglomeration or segregation due to better wettability from copper coating on B_4C. Copper coating of B_4C particles ensures optimum matrix-reinforcement interaction, transferring load/force to the matrix material and strengthening the composite. With increasing dislocation density, more uniform B_4C particles strengthen. B_4C particles cause dislocation pile-ups, restricting soft matrix material plastic flow and strengthening it.

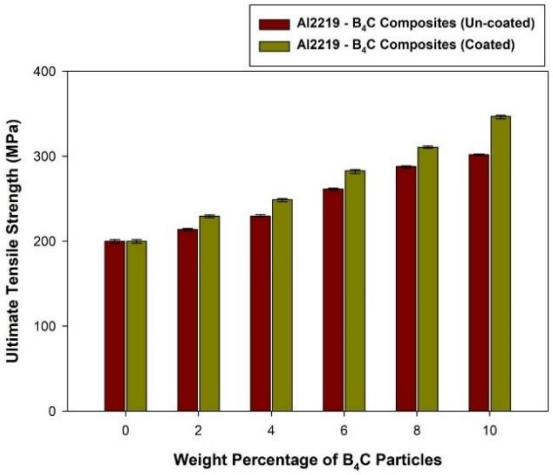

Fig. 15. UTS of Al2219 alloy compared to B_4C composites with reinforcement that are uncoated and coated with Cu

Figure 16 shows that uncoated B_4C particles boost alloy yield strength. Al2219 alloy yield strength increases as uncoated B_4C particles grow from 2 to 10%. YS of 165.48 MPa rises to 175.2 MPa in B_4C-reinforced Al2219 alloys with 2, 4, 6, 8, and 10 weight percent B_4C. Al2219 at 10 wt% increases the yield strength of uncoated B_4C composites by 46.01 percent. Hard B_4C particles have definitely boosted yield strength. This boosts structural rigidity, which is a plus. Cementation may have caused a catastrophic, persistent compression failure due to the expansion of the brittle particles, which have different expansion coefficients than the flexible matrix [34, 35]. The tight packing of stiffeners and narrow grid particle spacing further improves quality. Youming Luo [36] and co-authors studied the impact of copper-coated graphene particles on the mechanical behaviour of aluminium composites; with these particles, superior properties were obtained.

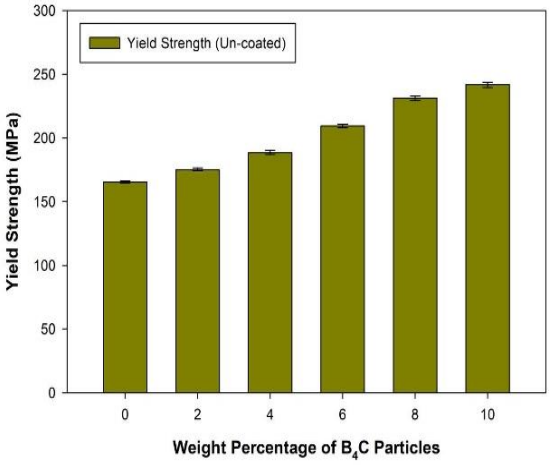

Fig. 16. Yield strength of Al2219 alloy reinforcement of B_4C particle composites without coating

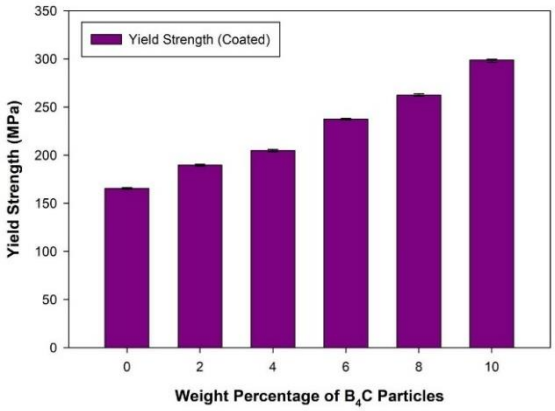

Fig. 17. Displays the yield strength of composites made from Al2219 alloy, which have been strengthened by B4C particles that are coated in Cu.

Figure 17 shows alloy Al2219 with 2, 4, 6, 8, or 10% Cu-coated Reinforcement of composites with B_4C particles. Figure 17 indicates that Al2219 yield strength rises from 2 to 10% Cu-coated B_4C particles. Al2219 alloy with 2–10 wt. % Cu coated B_4C reinforced composites have 165.48 MPa, while with 10% Cu coated B_4C, it has 189.47, 204.77, 237.23, 262.55, and 298.09 MPa. Enhancing the wettability of the matrix and reinforcement through a two-stage stir casting process utilising a boron carbide particle coating. Distributing particles evenly throughout the matrix reduces plastic deformation [37, 38].

Figure 18 presents an assessment of the yield strength of Al2219 with composites reinforced by uncoated and coated B4C particles. The composites were created using different weight proportions of 2, 4, 6, 8, and 10. The yield strength of uncoated and Cu-coated B_4C reinforced composites rises as particle weight increases from 2 to 10 wt.%. The YS of alloy 2219 is 165.48 MPa when cast, but adding 10% uncoated B_4C particles raises it to 241.62 MPa. Cu-coated B_4C reinforcement of composites with particles increases yield strength. The reinforcement of composites with Cu-coated B4C had a higher yield strength compared to the reinforcement of composites with uncoated particles (Figure 18). Al2219 – 10% Cu coated B_4C reinforced composite yields 298.09 MPa. With 10 wt.% uncoated and Cu-coated B_4C composites with reinforcement, the Al2219 alloy YS was enhanced by 46.01% and 80.13% respectively. Cu-coated Al2219 alloy particles bind the aluminium matrix and ceramic particles, making them stronger than uncoated composites. Particles coated in Cu. The Ramesh et al. [39] investigation of Ni-P-coated Al6061-Si3N4 composites exhibited the same pattern.

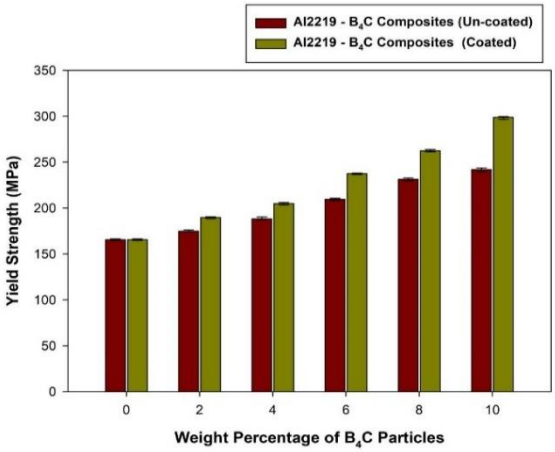

Fig. 18. Displays the yield strength (YS) comparison of Al2219 alloy in B_4C reinforced composites, both uncoated and coated with Cu.

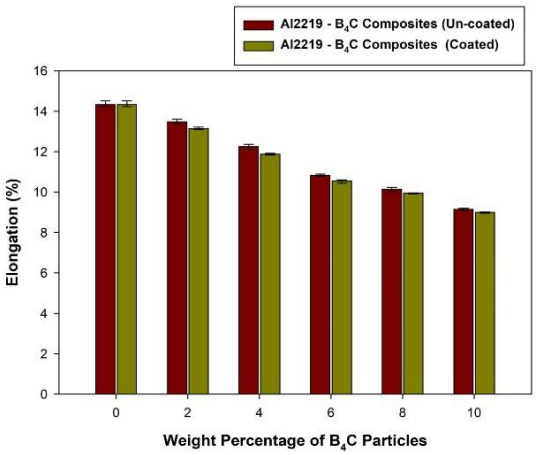

Fig. 19. Displays the comparison of the % elongation of Al2219 alloy in two distinct states: uncoated and Cu coated B_4C reinforced composites.

Figure 19 illustrates the comparison of Al2219 elongation with different weight percentages (2%, 4%, 6%, 8%, and 10%) of uncoated and Cu-coated B_4C particle reinforced composites. As particle weight percent rises from 2 to 10 weight percent, Al2219 alloy elongation decreases in uncoated and Cu-coated B4C reinforcement with particle composites. The reduction in extension is attributed to the combination of ceramic particles into the Al2219 soft aluminium matrix. The plasticity of the aluminium matrix goes down as the proportion of the matrix's hard particles rises. As the mass percentage of boron carbide particles goes from 2% to 10%, the ductility of Al2219-B_4C composites goes down. This is because the hard reinforcement particles become more brittle. The composites containing B_4C particles coated with Cu and uncoated B_4C particles in Al2219 alloy show similar ductility, with the Cu-coated composites exhibiting slightly lower ductility. Cu coating on ceramic particles modifies the surface and improves matrix bonding, decreasing ductility [40, 41].

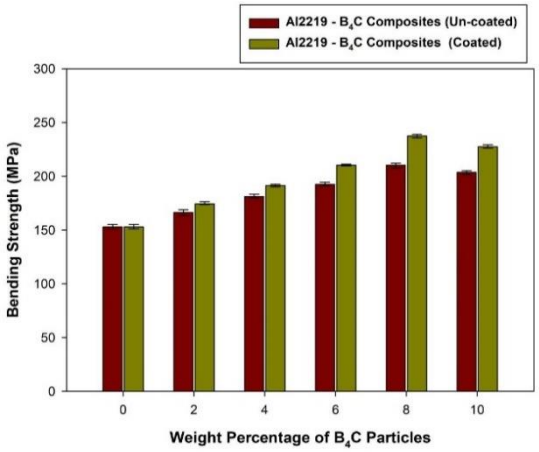

Fig. 20 compares the bending strength of Al2219 alloy in B_4C reinforced composites with and without Cu coating.

Figure 20 illustrates a comparison between the bending strength of Al2219 alloy and how strong an uncoated object can bend and Cu-coated B_4C reinforced composites. The accumulation of uncoated and Cu-coated B_4C particles to Al2219 composites increases their bending strength by 2–10%. The composites fabricated using Al2219 alloy with Cu-coated B4C particles demonstrate enhanced flexural strength in comparison to both the uncoated particles and the original matrix in its initial cast condition. The strength to bend of the Al2219 alloy is 153.13 MPa. The bending strength of the Al2219 alloy improves as the percentage of weight of uncoated and Cu-coated B_4C particles increases. The Al2219 composite material, reinforced by 10% uncoated B_4C particles, exhibits a bending strength of 203.3 MPa. The composite, consisting of B_4C reinforcement with particles of Al2219 alloy containing 10 wt. % Cu coating exhibits a bending strength of 227.6 MPa. Uncoated and Cu-coated B_4C particles boost Al2219's bending strength by 32.6% and 48%, respectively. Cu coated B_4C reinforcement with particle composites has higher bending strength due to their resistance to debonding during bending stress. De-bonding of uncoated particles is more likely in composites with comparatively uncoated particles, reducing bending strength compared to Cu-coated B_4C particles.

3.5. Tensile Fractography

Figures 21 (a-c) represent the tensile fractured surfaces of as-cast Al2219 (Fig. 21a), Al2219 with 10 wt.% of uncoated B4C composites (Fig. 21b), and Al2219 with 10 wt.% of Cu-coated B_4C composites (Fig. 21c), respectively. The fractured surface of an as-cast alloy indicates clear grains with a ductile mode of fracture. This can be with respect to the large deformation during the tensile loading.

Figures 21 (b, c) are fractured surfaces of uncoated and coated B4C particle composites. Tensile fractured surfaces contain the boron carbide particles on the surfaces, a very difficult and very rare phenomenon to occur in metal composites. Reinforcement presence occurs in the metal composites if only strong interfacial bonding exists between the base and particles. Further, in the present investigations, from Fig. 21 (c), strong interfacial bonding is observed between the Al2219 matrix and B_4C particles. The existence of a strong bond is due to the presence of copper on the surface of the particle. This copper coating helps in bringing the metal to the metal surface in contact instead of ceramic-metal contact. Al2219 alloy with 10 wt. % of uncoated and copper-coated B_4C particle composites showed a brittle mode of fracture on the surface, and some places exhibited a ductile mode. The copper-coated particle composites indicate very high interfacial bonding, which is clearly indicated in Fig. 21 (c), in which particle shear occurred during the tensile loading.

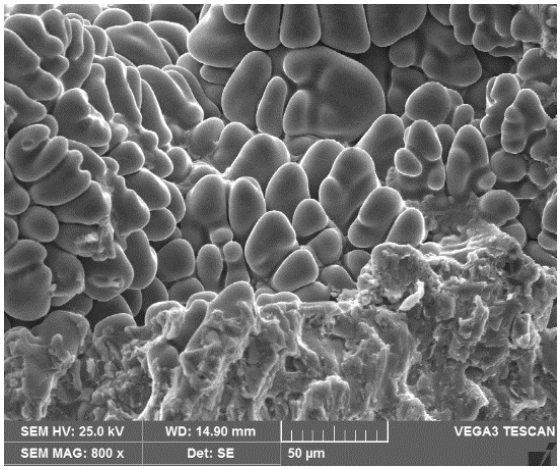

(a)

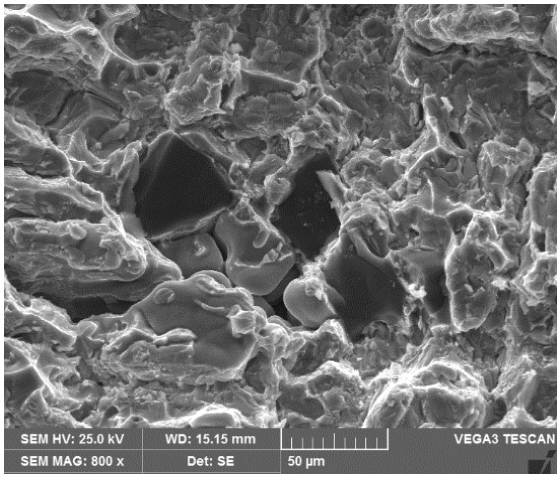

(b)

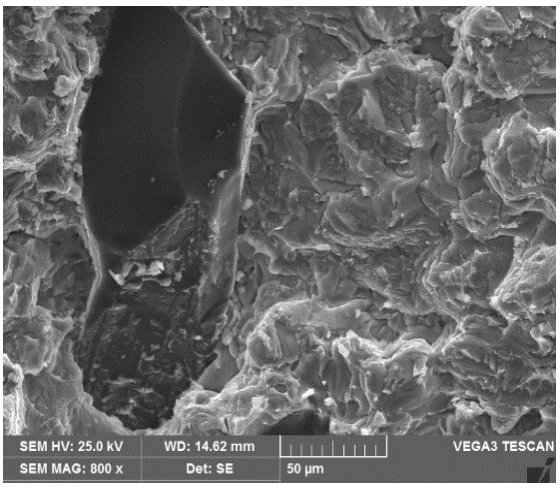

(c)

Fig. 21. Tensile fractured surfaces of: (a) as-cast Al2219, (b) Al2219 with 10 wt. % of un-caoted B_4C composites, (c) Al2219 with 10 wt. % of Cu-caoted B_4C composites

4. Conclusions

- In the current work, composite materials were generated by mixing Al2219 alloys with 80-90 micron uncoated and copper-coated B4C particles, and then stirring the mixture.
- Microstructures and qualities, including density, hardness, tensile, and bending, were examined in alloy 2219 metal composites.
- The microstructure shows a homogeneous distribution of Cu-Coated B_4C microparticles in the produced composite as compared to the uncoated B_4C Particles.
- The EDS results show boron carbide particle phases in the Al2219 alloy matrix.
- The Al2219 alloy had lower hardness, tensile strength, and bending strength than copper-coated B_4C composite materials strengthened by the addition of particles with 85-90 microns. Metal composites were a little less dense than Al2219.
- The strong interfacial bonding is presented in the case of copper-coated B_4C particle-reinforced composites. Al2219 alloy showed a ductile mode of fracture with more ductility, and brittle fracture surfaces were found in the boron carbide particle composites.

Funding Statement

This research did not receive any specific grant from funding agencies in the public, commercial, or not-for-profit sectors.

Conflicts of Interest

The author declares that there is no conflict of interest regarding the publication of this article.

References

[1] Nikhil, G., Nguyen, Q. and Pradeep, K.R., 2011. Analysis of active cooling through nickel-coated carbon fibers in the solidification processing of aluminium matrix composites. *Composites Part B*, 42, pp. 916-925.

[2] Bharath, V., Nagaral, M. and Auradi, V., 2012. Preparation of 6061Al-Al2O3 metal matrix composite by stir casting and evaluation of mechanical properties. International *Journal of Metallurgical & Materials Science* and Engineering, 2(3), pp. 22-31.

[3] Nagaral, M., Auradi, V. and Kori, S. A., 2015. Microstructure and mechanical properties of Al6061-Graphite composites fabricated by stir casting process. *Applied Mechanics and Materials,* 766, pp. 308-314.

[4] Zulfia, A., Putro, E.C., Wahyudi, M.D. and Daneshwara, B.W., 2018. Fabrication and characteristics of ADC-12 reinforced nano SiC and nano Al_2O_3 composites through stir casting route. *IOP Conference Series: Materials Science and Engineering,* 432, 012032.

[5] Canakci, A., Arslan, F. and Yasar, I., 2007. Pre-treatment process of B_4C particles to improve incorporation into molten AA2014 alloy. *Journal of Materials Science,* 42, pp.9536–9542.

[6] Raj, K., Deshpande, R.G., Gopinath, P., Jayasheel, H., Nagaral, M. and Auradi, V., 2011. Mechanical Fractography and Worn Surface Analysis of Nanographite and ZrO2-Reinforced Al7075 Alloy Aerospace Metal Composites. *Journal of Failure Analysis and Prevention,* 21, pp. 525-536.

[7] Pankaj, R.J., Sridhar, B.R., Nagaral, M. and Jayasheel, I.H., 2017. Evaluation of mechanical properties of B_4C and graphite particulates reinforced A356 alloy hybrid composites. *Materials Today: Proceedings,* 4(9), pp. 9972-9976.

[8] Clement, T.S. and Pugazhenthi, R., 2021. Effect of process parameter on synthesizing of TiC reinforced Al7075 aluminium alloy nano composites. *Materials Today Proceedings,* 37(2), pp. 1978-1981.

[9] Satish, B.B., Samuel, D., Bharath, V.M., Nagaral, M., Aravinda, T., Vijee, K. and Virupaxi, A., 2021. Development and Mechanical Characterisation of Al6061-Al_2O_3-Graphene Hybrid Metal Matrix Composites. *Journal of Composites Science,* 5(6), pp. 155.

[10] Siddesh, M., Shivakumar, B.P., Shashidhar, S. and Nagaral, M., 2021. Dry sliding wear behavior of mica, fly ash and red mud particles reinforced Al7075 alloy hybrid metal matrix composites. *Indian Journal of Science and Technology*, 14(4), pp. 310-318.

[11] Umanath, K., Selvamani, S.T., Palanikumar, K., Raphael, T. and Prashanth, K., 2013. Effect of sliding distance on dry sliding wear behavior of Al6061-SiC-Al_2O_3 hybrid composite. *Proceedings of International Conference on Advances in Mechanical Engineering,* pp. 749-75.

[12] Nagaral, M., Vijaykumar, H., Auradi, V., Kori, S. A., 2018. Influence of Two-Stage Stir Casting Process on Mechanical Characterization and Wear Behavior of AA2014-ZrO_2 Nano-composites. *Transactions of the Indian Institute of Metals,* 71, pp. 2845-2850.

[13] Veeresh Kumar, G.B., Gude, V.C., Mandadi, S.V., Jayarami, R.K., Nagaral, M. and Naresh, K., 2022. Effects of addition of Titanium Diboride and Graphite Particulate Reinforcements on physical, mechanical and tribological properties of Al6061 Alloy based Hybrid Metal Matrix Composites. *Advances in Materials and Processing Technologies,* 8(2), pp. 2259-2276.

[14] Bharath, V., Auradi, V., Nagaral, M. and Satish,B.B., 2020. Experimental Investigations on Mechanical and Wear Behaviour of 2014Al–Al_2O_3 Composites. *Journal of Bio-and Tribo-Corrosion*, 6, pp. 1-10.

[15] Nagaral, M., Auradi, V., Parashivamurthy, K.I., Kori, and S. A. Shivananda, B.K., 2018. Synthesis and characterization of Al6061-SiC-graphite composites fabricated by liquid metallurgy. *Materials Today: Proceedings,* 5(1), pp. 2836-2843.

[16] Gopal Krishna, U.B., Vasudeva, B., Virupaxi, A. and Nagaral, M., 2021. Effect of percentage variation on wear behaviour of

tungsten carbide and cobalt reinforced Al7075 matrix composites synthesized by melt stirring method. *Journal of Bio-and Tribo-Corrosion,* 7(3), pp. 89.

[17] Bharath, V., Auradi, V., Nagaral, M., Satish, B.B., Ramesh, S. and Palanikumar, K., 2021. Microstructural and wear behavior of Al2014-alumina composites with varying alumina content. *Transactions of the Indian Institute of Metals*, 75, pp. 133-147.

[18] Vasanth Kumar, H.S., Kempaiah, U.N., Nagaral, M. and Revanna, K., 2021. Investigations on mechanical behaviour of micro B_4C particles reinforced Al6061 alloy metal composites. *Indian Journal of Science and Technology,* 14(22), pp. 1855-1863.

[19] Sampath, K.R., Chittappa, H.C. and Nagaral, M., 2025. Influence graphite and ZrO_2 particles addition on the mechanical and wear behavior of Al7075 alloy composites. *Journal of Bio and Tribo Corrosion*, 11(3), pp. 92.

[20] Zeeshan, A., Muthuraman, V., Rathnakumar, P., Gurusamy, P. and Nagaral, M., 2022. Studies on mechanical properties of 3 wt% of 40 and 90 μm size B_4C particulates reinforced A356 alloy composites. *Materials Today: Proceedings,* 52, pp. 494-499.

[21] Pathalinga, G.P., Chittappa, H.C., Nagaral, M. and Auradi, V., 2020. Influence of B_4C Reinforcement Particles with Varying Sizes on the Tensile Failure and Fractography of LM29 Alloy Composites. *Journal of Failure Analysis and Prevention,* 20(6), pp. 2078-2086.

[22] Samuel, D., Satish, B.B., Auradi, V., Nagaral, M., Udaya, R.M., Bharath, V., 2021. Evaluation of Wear Properties of Heat-Treated Al-AlB_2 in-situ Metal Matrix Composites. *Journal of Bio-and Tribo-Corrosion*, 7(40), pp. 1-11.

[23] Nagaraj, N., Mahendra, K.V. and Nagaral, M., 2018. Microstructure and evaluation of mechanical properties of Al-7Si-fly ash composites. Materials Today: Proceedings, 5(1), pp. 3109-3116.

[24] Fazil, N., Venkataramana, V., Nagaral, M. and Auradi, V., 2018. Synthesis and mechanical characterization of micro B4C particulates reinforced AA2124 alloy composites. *International Journal of Engineering and Technology UAE,* 7(2.23), pp. 225-229.

[25] Balaraj, V., Nagaraj, K., Nagaral, M. and Auradi, V., 2021. Microstructural evolution and mechanical characterization of micro Al_{2O3} particles reinforced Al6061 alloy metal composites. *Materials Today: Proceedings, 4*7, pp. 5959-5965.

[26] Manjunatha, T.H., Yadavalli, B., Nagaral, M., Venkataramana, V. and Jayasheel, I. H., 2018. Investigations on mechanical behavior of Al7075-nano B_4C composites. *IOP Conference Series: Materials Science and Engineering*, 376(1), 012091.

[27] Krishna, P.S., Samuel, D., Rajesh, M., Nagaral, M., Auradi, V. and Rabin, S., 2022. Preparation and mechanical characterization of TiC particles reinforced Al7075 alloy composites. *Advances in Materials Science and Engineering,* 7105189.

[28] Pankaj, R.J., Nagaral, M., Shivakumar, R. and Jayasheel, I.H., 2020. Impact of boron carbide and graphite dual particulates addition on wear behavior of A356 alloy metal matrix composites. *Journal of Metals, Materials and Minerals,* 30(4), pp. 106-112.

[29] Bharath, V., Auradi, V., Veeresh Kumar, G.B., Nagaral, M., Murthy, C., Mahmoud, H., Rokayya, S., Aljuraide, N.I., Jong, W.H. and Ahmed, M.G., 2022. Microstructural Evolution, Tensile Failure, Fatigue Behavior and Wear Properties of Al2O3 Reinforced Al2014 Alloy T6 Heat Treated Metal Composites. *Materials,* 15(12), 4244.

[30] Priyankar, D., Zeeshan, A., Nagaral, M., Rathnakumar, P., Muthuraman, V. and Umar, M.D., 2022. Microstructure and evolution of mechanical properties of Cu-Sn alloy with graphite and nano zirconium oxide particulates. *Materials Today: Proceedings*, 52, pp. 296-300.

[31] Vasanth Kumar, H.S., Kempaiah, U.N., Nagaral, M. and Auradi, V., 2021. Impact, tensile and fatigue failure analysis of boron carbide particles reinforced Al-Mg-Si (Al6061) alloy composites. *Journal of Failure Analysis and Prevention,* 21(6), pp. 2177-2189.

[32] Angadi, S.B., Sntosh, K., Nagaral, M., Auradi, V. and Balaraj, V., 2025. Effect of ceramic boron carbide particles addition on the mechanical and microstructural characteristics Al7020 Alloy composites. *Mechanics of Advanced Composite Structures,* 12(1), pp. 169-180.

[33] Bharath, V., Virupaxi, A., Nagaral, M., Manjunath, V., Nagaraj, N., Chandrashekar, A., Shanawaz, P., Abdul, R., Abdullah, H.A., Shamshad, A. and Mohammad, O.Q., 2023. Al2014–alumina aerospace composites: particle size impacts on microstructure,

mechanical, fractography, and wear characteristics. *ACS omega*, 8(14), pp. 13444-13455.

[34] Rashmi, P.S., Mahesh, T.S., Zeeshan, A., Veeresha, G. and Nagaral, M., 2022. Studies on mechanical behaviour and tensile fractography of boron carbide particles reinforced Al8081 alloy advanced metal composites. *Materials Today: Proceedings*, 52, pp. 2115-2120.

[35] Gorad, S.R., Satish, B.B., Samuel, D., Nagaral, M. and Auradi, V., 2024. Microstructure, mechanical behavior, and tensile fractography of Si3N4-reinforced Al2219 alloy composites synthesized by squeeze casting method. *Journal of Failure Analysis and Prevention.* https://doi.org/10.1007/s11668-024-01956-0.

[36] Youming, L., Yaling, H. and Jie, L., 2023. Quanfang Chen, Copper coated graphene reinforced aluminium composites with enhanced mechanical strength and conductivity. *Vacuum,* 218, 112610.

[37] Rashmi, P.S., Hemanth Raju, T.H., Nagaral, M., Nithin, K. and Auradi, V., 2024. Effect of B_4C particles addition on the mechanical, tensile fracture and wear Behavior of Al7075 alloy composites. *Journal of Bio-and Tribo-Corrosion,* 10(2), p.32.

[38] Subbaraya, M.K., Mahendra, K.V., Bharatish, A., Manjunatha, B., Nagaraj, N. and Nagaral, M., 2024. Impact on casting die diameter size on microstructure and fractographic studies of Al-2024 alloy reinforced with fly ash and SiC Hybrid Composites. *Applied Research,* 3(4), p.e202300066.

[39] Ramesh, C.S., Keshavamurthy, R., Channabasappa, B.H. and Ahmed, A., 2009. Microstructure and mechanical properties of Ni–P coated Si3N4 reinforced Al6061 composites. *Materials Science and Engineering: A,* 502(1-2), pp.99-106.

[40] Raksha, M.S., Nagaral, M., Satish, B.B., Chandrashekar, A., Mohammad, S., Mohammed, O., Saiful, I., Vivek, B., Rohini, K.P., Mohammad, A.K. and Abdul, R., 2023. Impact of boron carbide particles and weight percentage on the mechanical and wear characterization of Al2011 alloy metal composites. *ACS Omega*, 8(26), pp. 23763-23771.

[41] Ali, Z., Muthuraman, V., Rathnakumar, P., Gurusamy, P. and Nagaral, M., 2023. Influence of B_4C particle size on the mechanical behaviour of A356 aluminium composites. *Research on Engineering Structures and Materials*, 9(2), pp. 527-540.